

Many-Body Dynamics of Exciton Creation in a Quantum Dot by Optical Absorption: A Quantum Quench towards Kondo Correlations

Hakan E. Türeci,^{1,2} M. Hanl,³ M. Claassen,² A. Weichselbaum,³ T. Hecht,³ B. Braunecker,⁴ A. Govorov,⁵ L. Glazman,⁶ A. Imamoglu,² and J. von Delft³

¹*Department of Electrical Engineering, Princeton University, Princeton, New Jersey 08544, USA*

²*Institute for Quantum Electronics, ETH-Zürich, CH-8093 Zürich, Switzerland*

³*Arnold Sommerfeld Center for Theoretical Physics, Ludwig-Maximilians-Universität München, D-80333 München, Germany*

⁴*Department of Physics, University of Basel, Klingelbergstrasse 82, 4056 Basel, Switzerland*

⁵*Department of Physics and Astronomy, Ohio University, Athens, Ohio 45701, USA*

⁶*Sloane Physics Laboratory, Yale University, New Haven, Connecticut 06520, USA*

(Received 14 May 2010; published 9 March 2011)

We study a quantum quench for a semiconductor quantum dot coupled to a Fermionic reservoir, induced by the sudden creation of an exciton via optical absorption. The subsequent emergence of correlations between spin degrees of freedom of dot and reservoir, culminating in the Kondo effect, can be read off from the absorption line shape and understood in terms of the three fixed points of the single-impurity Anderson model. At low temperatures the line shape is dominated by a power-law singularity, with an exponent that depends on gate voltage and, in a universal, asymmetric fashion, on magnetic field, indicative of a tunable Anderson orthogonality catastrophe.

DOI: 10.1103/PhysRevLett.106.107402

PACS numbers: 78.67.Hc, 78.40.Fy, 78.60.Fi

When a quantum dot (QD) is tunnel coupled to a Fermionic reservoir (FR) and tuned such that its topmost occupied level harbors a single electron, it exhibits at low temperatures the Kondo effect, in which QD and FR are bound into a spin singlet. It is interesting to ask how Kondo correlations set in after a quantum quench, i.e., a sudden change of the QD Hamiltonian, and corresponding predictions have been made in the context of transport experiments [1–4]. Optical transitions in quantum dots [5–7] offer an alternative arena for probing Kondo quenches: the creation of a bound electron-hole pair—an exciton—via photon absorption implies a sudden change in the local charge configuration. This induces a sudden switch-on of both a strong electron-hole attraction [6–8] and an exchange interaction between the bound electron and the FR. The subsequent dynamics is governed by energy scales that become ever lower with increasing time, leaving tell-tale signatures in the absorption and emission line shapes. For example, at low temperatures and small detunings relative to the threshold, the line shape has been predicted to show a gate-tunable power-law singularity [8]. Though optical signatures of Kondo correlations have not yet been experimentally observed, prospects for achieving this goal improved recently due to two key experimental advances [9,10].

Here we propose a realistic scenario for an optically induced quantum quench into a regime of strong Kondo correlations. A quantum dot tunnel coupled to a FR is prepared in an uncorrelated initial state [Fig. 1(a)]. Optical absorption of a photon creates an exciton, thereby inducing a quantum quench to a state conducive to Kondo correlations [Fig. 1(b)]. The subsequent emergence of spin

correlations between the QD-electron and the FR, leading to a screened spin singlet, is imprinted on the optical absorption line shape [Fig. 1(c)]: its high-, intermediate-, and low-detuning behaviors are governed by the three fixed points of the single-impurity Anderson model (AM) [Fig. 1(d)]. We present detailed numerical and analytical results for the line shape as a function of temperature and magnetic field. At zero temperature we predict a tunable Anderson orthogonality catastrophe, since the difference in initial and final ground state phase shifts of FR electrons

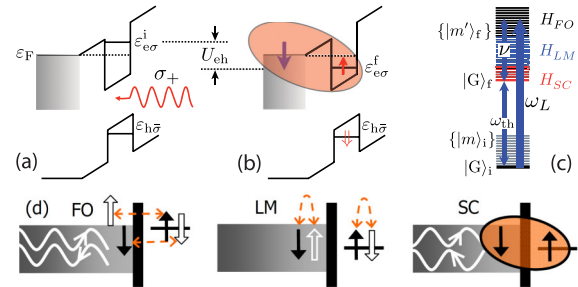


FIG. 1 (color online). A localized QD e level, tunnel coupled to a FR and (a) assumed empty at $t = 0$, (b) is filled at $t = 0^+$ when photon absorption produces a neutral exciton, leading to Kondo correlations between QD and FR for $t \rightarrow \infty$. (c) Starting from an empty QD state $|G\rangle_i$ (for $T = 0$), the absorption rate at frequency $\omega_L = \omega_{th} + \nu$ (with detuning ν from the threshold $\omega_{th} = E_G^f - E_G^i$) probes the spectrum of H^f at excitation energy ν . (d) Cartoons illustrating the nature of the free orbital (FO), local moment (LM) and strong-coupling (SC) fixed points of the Anderson impurity model, which are dominated by charge fluctuations, spin fluctuations (indicated by dashed arrows) and a screened spin singlet, respectively.

[indicated by wavy lines in Fig. 1(d)] can be tuned by magnetic field and gate voltage via their effects on the level occupancy.

Model.—We consider a QD, tunnel coupled to a FR, whose charge state is controllable via an external gate voltage V_g applied between a top Schottky gate and the FR [see Fig. 1(a) and 1(b)]. In a gate voltage regime for which the QD is initially uncharged, a circularly polarized light beam (polarization σ) at a suitably chosen frequency ω_L propagating along the z axis of the heterostructure will create a so-called neutral exciton [11] (X^0), a bound electron-hole pair with well-defined spins σ and $\bar{\sigma} = -\sigma$ ($\in \{+, -\}$) in the lowest available localized s orbitals of the QD's conduction- and valence bands (to be called e and h levels, with creation operators e_σ^\dagger and $h_{\bar{\sigma}}^\dagger$, respectively). The QD-light interaction is described by $H_L \propto (e_\sigma^\dagger h_{\bar{\sigma}}^\dagger e^{-i\omega_L t} + \text{H.c.})$. We model the system before and after absorption by the initial and final Hamiltonian $H^{i/f} = H_e^{i/f} + H_c + H_t$, where

$$H_e^a = \sum_\sigma \varepsilon_{e\sigma}^a n_{e\sigma} + U n_{e\uparrow} n_{e\downarrow} + \delta_{af} \varepsilon_{h\bar{\sigma}} \quad (a = i, f) \quad (1)$$

describes the QD, with Coulomb cost U for double occupancy of the e level, $n_{e\sigma} = e_\sigma^\dagger e_\sigma$, and hole energy $\varepsilon_{h\bar{\sigma}} (> 0$, on the order of the band gap). The e level's initial and final energies before and after absorption, $\varepsilon_{e\sigma}^a$ ($a = i, f$), differ by the Coulomb attraction $U_{\text{ch}} (> 0)$ between the newly created electron-hole pair, which pulls the final e level downward, $\varepsilon_{e\sigma}^f = \varepsilon_{e\sigma} - \delta_{af} U_{\text{ch}}$ [Fig. 1(b)]. This stabilizes the excited electron against decay into the FR, provided that $\varepsilon_{e\sigma}^f$ lies below the FR's Fermi energy $\varepsilon_F = 0$. Since $H^f \neq H^i$, absorption implements a quantum quench, which, as elaborated below, can be tuned by electric and magnetic fields. The term $H_c = \sum_{k\sigma} \varepsilon_{k\sigma} c_{k\sigma}^\dagger c_{k\sigma}$ represents a noninteracting conduction band (the FR) with half-width $D = 1/(2\rho)$ and constant density of states ρ per spin, while $H_t = \sqrt{\Gamma/\pi\rho} \sum_\sigma (e_\sigma^\dagger c_\sigma + \text{H.c.})$, with $c_\sigma = \sum_k c_{k\sigma}$, describes its tunnel coupling to the e level, giving it a width Γ . A magnetic field B along the growth-direction of the heterostructure (Faraday configuration) causes a Zeeman splitting, $\varepsilon_{e\sigma} = \varepsilon_e + \frac{1}{2} \sigma g_e B$, $\varepsilon_{h\sigma} = \varepsilon_h + \frac{3}{2} \sigma g_h B$ (the Zeeman splitting of FR states can be neglected for our purposes [12]). The electron-hole pair created by photon absorption will additionally experience a weak but highly anisotropic intradot exchange interaction [12]. Its effects can be fully compensated by applying a magnetic field fine-tuned to a value, say B_{ch}^σ , that restores degeneracy of the e level's two spin configurations [12]. Henceforth, B is understood to be measured relative to B_{ch}^σ . We set $\mu_B = \hbar = k_B = 1$, give energies in units of $D = 1$ throughout, and assume $T, B \ll \Gamma \ll U, U_{\text{ch}} \ll D \ll \varepsilon_{h\bar{\sigma}}$. The electron-hole recombination rate is assumed to be negligibly small compared to all other energy scales. We focus on the case, illustrated in

Figs. 1(a) and 1(b), where the e level is essentially empty in the initial state and singly occupied in the ground state of the final Hamiltonian, $\bar{n}_e^i \approx 0$ and $\bar{n}_e^f \approx 1$. (Here $\bar{n}_e^a = \sum_\sigma \bar{n}_{e\sigma}^a$, and $\bar{n}_{e\sigma}^a = \langle n_{e\sigma} \rangle_a$ is the thermal average of $n_{e\sigma}$ with respect to H^a .) This requires $\varepsilon_{e\sigma}^i \gg \Gamma$, and $-U + \Gamma \lesssim \varepsilon_{e\sigma}^f \lesssim -\Gamma$. The Kondo temperature associated with H^f is $T_K = \sqrt{\Gamma U/2} e^{-\pi|\varepsilon_e^f(\varepsilon_e^f + U)|/(2U\Gamma)}$. If $\varepsilon_{e\sigma}^f = -U/2$, so that $\bar{n}_e^f = 1$, then H^f represents the symmetric excitonic Anderson model, to be denoted by writing $H^f = \text{SEAM}$.

Absorption line shape.—Absorption sets in once ω_L exceeds a threshold frequency, ω_{th} . The line shape at temperature T and detuning $\nu = \omega_L - \omega_{\text{th}}$ is, by the golden rule, proportional to the spectral function (see [13])

$$A_\sigma(\nu) = 2\pi \sum_{mm'} \rho_m^i |{}_f \langle m' | e_\sigma^\dagger | m \rangle_i|^2 \delta(\omega_L - E_{m'}^f + E_m^i). \quad (2)$$

Here $|m\rangle_a$ and E_m^a are exact eigenstates and energies of H^a , depicted schematically in Fig. 1(c), and $\rho_m^i = e^{-E_m^i/T}/Z^i$ the initial Boltzmann weights. The threshold frequency evidently is $\omega_{\text{th}} = E_G^f - E_G^i$ (E_G^a is the ground state energy of H^a), which is on the order of $\varepsilon_{e\sigma}^f + \varepsilon_{h\bar{\sigma}}$ (up to corrections due to tunneling and correlations).

We calculated $A_\sigma(\nu)$ using the Numerical Renormalization Group (NRG) [14], generalizing the approach of Refs. [8,15] to $T \neq 0$ by following Ref. [16]. The inset of Fig. 2 shows a typical result: As temperature is gradually reduced, an initially rather symmetric line shape becomes highly asymmetric, dramatically increasing in peak height as $T \rightarrow 0$. At $T = 0$, the line shape displays a threshold, vanishing for $\nu < 0$ and diverging as ν tends to 0 from above. Figure 2 analyzes this divergence on a log-log plot, for the case that T , which cuts off the divergence, is smaller than all other relevant energy scales. Three distinct functional forms emerge in the regimes of ‘‘large’’, ‘‘intermediate’’ or ‘‘small’’ detuning, labeled (for reasons discussed below) FO, LM and SC, respectively, (given here for $H^f = \text{SEAM}$):

$$|\varepsilon_{e\sigma}^f| \lesssim \nu \lesssim D: \quad A_\sigma^{\text{FO}}(\nu) = \frac{4\Gamma}{\nu^2} \theta(\nu - |\varepsilon_{e\sigma}^f|); \quad (3a)$$

$$T_K \lesssim \nu \lesssim |\varepsilon_{e\sigma}^f|: \quad A_\sigma^{\text{LM}}(\nu) = \frac{3\pi}{4\nu} \ln^{-2}(\nu/T_K); \quad (3b)$$

$$T \lesssim \nu \lesssim T_K: \quad A_\sigma^{\text{SC}}(\nu) \propto T_K^{-1} (\nu/T_K)^{-\eta_\sigma}. \quad (3c)$$

The remarkable series of crossovers found above are symptomatic of three different regimes of charge and spin dynamics. They can be understood analytically using fixed-point perturbation theory (FPPT). To this end, note that at $T = 0$ the absorption line shape can be written as

$$A_\sigma(\nu) = 2 \text{Re} \int_0^\infty dt e^{i\nu t} \langle G | e^{i\bar{H}t} e_{e\sigma} e^{-i\bar{H}t} e_\sigma^\dagger | G \rangle_i, \quad (4)$$

where $\bar{H}^a = H^a - E_G^a$ and $\nu_+ = \nu + i0_+$. Thus it directly probes the postquench dynamics, with initial state $e_\sigma^\dagger |G\rangle_i$,

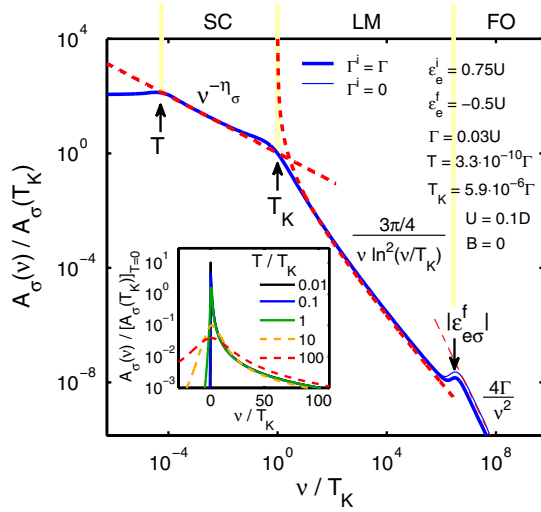


FIG. 2 (color online). Log-log plot of the absorption line shape $A_\sigma(\nu)$ for $T \ll T_K$, $B = 0$ and $H^f = \text{SEAM}$ (for which $\eta_\sigma = \frac{1}{2}$), showing three distinct functional forms for high, intermediate and small detuning, labeled FO, LM, and SC, respectively, according to the corresponding fixed points of the Anderson model. Arrows indicate the crossover scales T , T_K and $|\varepsilon_{e\sigma}^f|$. Fixed-point perturbation theory [FPPT, red dashed lines, from Eq. (3)] and NRG (thick blue line for $\Gamma_i \neq 0$; thin blue line for $\Gamma_i = 0$) agree well. Inset: $A_\sigma(\nu)$ for five temperatures in semilog scale, obtained from FPPT for $\Gamma_i = 0$ [dashed lines, from Eq. (7)] and NRG (solid lines).

of a photogenerated e -electron coupled to a FR. Evidently, large, intermediate or small detuning, corresponding to ever longer time scales after absorption, probes excitations at successively smaller energy scales [see Fig. 1(c)], for which \bar{H}^f can be represented by expansions $H_r^* + H_r'$ around the three well-known fixed points [14] of the AM: the free orbital, local moment and strong-coupling fixed points ($r = \text{FO, LM, SC}$), characterized by charge fluctuations, spin fluctuations and a screened spin singlet, respectively, as illustrated in Fig. 1(d).

Large and intermediate detuning—perturbative regime.—For large detuning, probing the time interval $t \lesssim 1/|\varepsilon_{e\sigma}^f|$ immediately after absorption, the e level appears as a free, filled orbital perturbed by charge fluctuations, described by [14] the fixed-point Hamiltonian $H_{\text{FO}}^* = H_c + H_e^f + \text{const}$ and the relevant perturbation $H_{\text{FO}}' = H_t$. Intermediate detuning probes the times $1/|\varepsilon_{e\sigma}^f| \lesssim t \lesssim 1/T_K$ for which real charge fluctuations have frozen out, resulting in a stable local moment; however, virtual charge fluctuations still cause the local moment to undergo spin fluctuations, which are not yet screened. This is described by [14] $H_{\text{LM}}^* = H_c + \text{const}$ and the RG-relevant perturbation $H_{\text{LM}}' = \frac{J(\nu)}{\rho} \vec{s}_e \cdot \vec{s}_c$. Here $\vec{s}_j = \frac{1}{2} \sum_{\sigma\sigma'} j_{\sigma\sigma'}^\dagger \vec{\tau}_{\sigma\sigma'} j_{\sigma\sigma'}$ (for $j = e, c$) are spin operators for the e level and conduction band, respectively, ($\vec{\tau}$ are Pauli matrices), and $J(\nu) = \ln^{-1}(\nu/T_K)$ is an effective, scale-dependent dimensionless exchange constant.

For $r = \text{FO}$ and LM, $A_\sigma(\nu)$ can be calculated using perturbation theory in H_r' . For $T = 0$, note that

$$A_\sigma(\nu) = -2 \text{Im}_i \langle G | e_\sigma \frac{1}{\nu_+ - \bar{H}^f} e_\sigma^\dagger | G \rangle_i, \quad (5)$$

set $\bar{H}^f \rightarrow H_r^* + H_r'$ and expand the resolvent in powers of H_r' . One readily finds (see [13])

$$A_\sigma^r(\nu) \simeq -\frac{2}{\nu^2} \text{Im}_i \langle G | e_\sigma H_r' \frac{1}{\nu_+ - H_r^*} H_r' e_\sigma^\dagger | G \rangle_i, \quad (6)$$

which reveals the relevant physics: Large detuning ($r = \text{FO}$) is described by the spectral function of the operator $H_r' e_\sigma^\dagger$; the absorption process can thus be understood as a two-step process consisting of a virtual excitation of the QD resonance, followed by a tunneling event to a final free-electron state above the Fermi level. In contrast, intermediate detuning ($r = \text{LM}$) is described by the spectral function of $\vec{s}_c \cdot \vec{s}_e e_\sigma^\dagger$, i.e., it probes spin fluctuations. Evaluating these spectral functions is elementary since H_{FO}^* and H_{LM}^* involve only free fermions. For $B = 0$ and $|\varepsilon_{e\sigma}^f| = \frac{1}{2}U$, we readily recover Eqs. (3a) and (3b) (see [13]), which quantitatively agree with the NRG results of Fig. 2.—Though the latter was calculated for $H^f = \text{SEAM}$, Eq. (3b) holds more generally as long as H^f remains in the LM regime, with $\bar{n}_e^f \simeq 1$; then $A_\sigma^{\text{LM}}(\nu)$ depends on $\varepsilon_{e\sigma}^f$, U and Γ only through their influence on T_K , and hence is a universal function of ν and T_K .

The FPPT strategy for calculating FO and LM line shapes can readily be generalized to finite temperatures [12], using the methods of Ref. [17] (Section III.A) for finding the finite- T dynamic magnetic susceptibility [13]. For $|\nu| \ll |\varepsilon_{e\sigma}^f|$ and $\max[|\nu|, T] \gg T_K$, we obtain

$$A_\sigma^{\text{LM}}(\nu) = \frac{3\pi}{4} \frac{\nu/T}{1 - e^{-\nu/T}} \frac{\gamma_{\text{Kor}}(\nu, T)/\pi}{\nu^2 + \gamma_{\text{Kor}}^2(\nu, T)}, \quad (7)$$

where $\gamma_{\text{Kor}}(\nu, T) = \pi T / \ln^2[\max(|\nu|, T)/T_K]$ is the scale-dependent Korringa relaxation rate [17]. It is smaller than T by a large logarithmic factor, implying a narrower and higher absorption peak than for thermal broadening.

Small detuning and Kondo-edge singularity—strong-coupling regime.—As ν is lowered through the bottom of the LM regime, $J(\nu)$ increases through unity into the strong-coupling regime, and $A_\sigma(\nu)$ monotonically crosses over to the SC regime. It was first studied for the present model (for $B = 0$) in Ref. [8], which found a power-law line shape of the form (3c), characteristic of a Fermi edge singularity, with an exponent η that followed Hopfield's rule [18]. The power-law behavior reflects Anderson orthogonality [19,20]: it arises because the final ground state $|G_f\rangle$ that is reached in the long-time limit is characterized by a screened singlet. The singlet ground state induces different phase shifts [as indicated in Fig. 1(d) by wavy lines] for FR electrons than the unscreened initial state just after photon absorption, $e_\sigma^\dagger |G_i\rangle$, and hence is orthogonal to the latter. It is straightforward to generalize

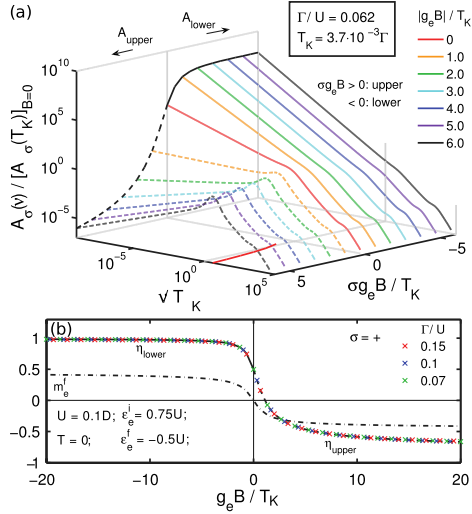


FIG. 3 (color online). Asymmetric magnetic-field dependence of the line shape for $H^f = \text{SEAM}$ and $T = 0$. (a) Depending on whether the electron is photoexcited into the lower or upper of the Zeeman-split e levels ($\sigma g_e B < 0$ or > 0 , solid or dashed lines, respectively), increasing $|B|$ causes the near-threshold divergence, $A_\sigma(\nu) \propto \nu^{-\eta_\sigma}$, to be either strengthened, or suppressed via the appearance of a peak at $\nu \approx \sigma g_e B$, respectively. (The peak's position is shown by the red line in the $\sigma g_e B$ - ν plane.) (b) Universal dependence on $g_e B/T_K$ of the local moment m_e^f (dash-dotted line), and the corresponding prediction of Hopfield's rule, Eq. (8), for the infrared exponents η_{lower} (solid line) and η_{upper} (dashed line) for $\sigma = +$. Symbols: η_+ values extracted from the near-threshold $\nu^{-\eta_+}$ divergence of $A_+(\nu)$. Symbols and lines agree to within 1%.

the arguments of Refs. [8,18] to the case of $B \neq 0$ (see [13]). One readily finds the generalized Hopfield rule

$$\eta_\sigma = 1 - \sum_{\sigma'} (\Delta n'_{e\sigma'})^2, \quad \Delta n'_{e\sigma'} = \delta_{\sigma\sigma'} - \Delta n_{e\sigma'}, \quad (8)$$

$\Delta n'_{e\sigma'}$ is the displaced charge of electrons with spin σ' , in units of e , that flows from the scattering site to infinity when $e_\sigma^\dagger |G_i\rangle$ is changed to $|G_f\rangle$, and $\Delta n_{e\sigma'} = \bar{n}_{e\sigma'}^f - \bar{n}_{e\sigma'}^i$ is the local occupation difference between $|G_f\rangle$ and $|G_i\rangle$.

According to Eq. (8), η_σ can be tuned not only via gate voltage but also via magnetic field, since both modify $\varepsilon_{e\sigma}^a$ and hence $\Delta n'_{e\sigma'}$. This tunability can be exploited to study universal aspects of Anderson orthogonality physics. In particular, if the system is tuned such that $\bar{n}_e^i = 0$ and $\bar{n}_e^f = 1$ at $B = 0$, Eq. (8) can be expressed as $\eta_\sigma = \frac{1}{2} + 2m_e^f \sigma - 2(m_e^f)^2$, where the final magnetization $m_e^f = \frac{1}{2} \times (\bar{n}_{e+}^f - \bar{n}_{e-}^f)$ is a universal function of $g_e B/T_K$. The exponents η_σ then are universal functions of $g_e B/T_K$, with simple limits for small and large fields [see Fig. 3(b)]: $\eta_\sigma \rightarrow \frac{1}{2}$ for $|g_e B| \ll T_K$, while $\eta_{\text{lower/upper}} \rightarrow \pm 1$ for $|g_e B| \gg T_K$. Here the subscript ‘‘lower’’ or ‘‘upper’’ distinguishes whether the spin- σ electron is photoexcited into the lower or upper of the Zeeman-split pair ($\sigma g_e B < 0$ or > 0 , respectively). The sign difference ± 1 for η_σ arises since these cases yield fully asymmetric changes in local

charge: $\Delta n_{e,\text{lower}} \rightarrow 1$ while $\Delta n_{e,\text{upper}} \rightarrow 0$. As a result, Anderson orthogonality [19] is completely absent ($\Delta n'_{e\sigma'} = 0$) for photo-excitation into the lower level, since subsequently the e -level spin need not adjust at all. In contrast, it is maximal ($\Delta n'_{e\sigma'} = 1$) for photo-excitation into the upper level, since subsequently the e -level spin has to create a spin-flip electron-hole pair excitation in the FR to reach its longtime value. It follows, remarkably, that a magnetic field tunes the strength of Anderson orthogonality, implying a dramatic asymmetry for the evolution of the line shape $A_\sigma(\nu) \propto \nu^{-\eta_\sigma}$ with increasing $|B|$ [Fig. 3(a)].

Conclusions.—We have shown that optical absorption in a single quantum dot can implement a quantum quench in an experimentally accessible solid-state system that allows the emergence of Kondo correlations and Anderson orthogonality to be studied in a tunable setting.

A. I. and H. E. T. acknowledge support from the Swiss NSF under Grant No. 200021-121757. H. E. T. acknowledges support from the Swiss NSF under Grant No. PP00P2-123519/1. B. B. acknowledges support from the Swiss NSF and NCCR Nanoscience (Basel). J. v. D. acknowledges support from the DFG (SFB631, SFB-TR12, De730/3-2, De730/4-1), the Cluster of Excellence NIM and in part from NSF under Grant No. PHY05-51164. A. I. acknowledges support from an ERC Advanced Investigator Grant, and L. G. from NSF Grant No. DMR-0906498.

- [1] P. Nordlander *et al.*, *Phys. Rev. Lett.* **83**, 808 (1999).
- [2] M. Plihal, D. C. Langreth, and P. Nordlander, *Phys. Rev. B* **71**, 165321 (2005).
- [3] F. B. Anders and A. Schiller, *Phys. Rev. Lett.* **95**, 196801 (2005).
- [4] D. Lobaskin and S. Kehrein, *Phys. Rev. B* **71**, 193303 (2005).
- [5] T. V. Shahbazyan, I. E. Perakis, and M. E. Raikh, *Phys. Rev. Lett.* **84**, 5896 (2000).
- [6] K. Kikoin and Y. Avishai, *Phys. Rev. B* **62**, 4647 (2000).
- [7] A. O. Govorov, K. Karrai, and R. J. Warburton, *Phys. Rev. B* **67**, 241307 (2003).
- [8] R. W. Helmes *et al.*, *Phys. Rev. B* **72**, 125301 (2005).
- [9] J. M. Smith *et al.*, *Phys. Rev. Lett.* **94**, 197402 (2005).
- [10] P. A. Dalgarno *et al.*, *Phys. Rev. Lett.* **100**, 176801 (2008).
- [11] A. Högele *et al.*, *Phys. Rev. Lett.* **93**, 217401 (2004).
- [12] H. Tureci *et al.* (to be published).
- [13] See supplemental material at <http://link.aps.org/supplemental/10.1103/PhysRevLett.106.107402>.
- [14] H. R. Krishna-murthy, J. W. Wilkins, and K. G. Wilson, *Phys. Rev. B* **21**, 1003 (1980).
- [15] T. A. Costi, *Phys. Rev. B* **55**, 3003 (1997).
- [16] A. Weichselbaum and J. von Delft, *Phys. Rev. Lett.* **99**, 076402 (2007).
- [17] M. Garst *et al.*, *Phys. Rev. B* **72**, 205125 (2005).
- [18] J. Hopfield, *Comments Solid State Phys.* **2**, 40 (1969).
- [19] P. W. Anderson, *Phys. Rev. Lett.* **18**, 1049 (1967).
- [20] P. Nozières and C. T. De Dominicis, *Phys. Rev.* **178**, 1097 (1969).